

# Accepted Manuscript

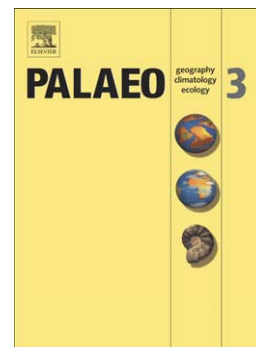
Arabia-Eurasia collision and the forcing of mid Cenozoic global cooling

Mark B. Allen, Howard A. Armstrong

PII: S0031-0182(08)00264-2  
DOI: doi: [10.1016/j.palaeo.2008.04.021](https://doi.org/10.1016/j.palaeo.2008.04.021)  
Reference: PALAEO 4714

To appear in: *Palaeogeography*

Received date: 22 August 2007  
Revised date: 11 March 2008  
Accepted date: 15 April 2008



Please cite this article as: Allen, Mark B., Armstrong, Howard A., Arabia-Eurasia collision and the forcing of mid Cenozoic global cooling, *Palaeogeography* (2008), doi: [10.1016/j.palaeo.2008.04.021](https://doi.org/10.1016/j.palaeo.2008.04.021)

This is a PDF file of an unedited manuscript that has been accepted for publication. As a service to our customers we are providing this early version of the manuscript. The manuscript will undergo copyediting, typesetting, and review of the resulting proof before it is published in its final form. Please note that during the production process errors may be discovered which could affect the content, and all legal disclaimers that apply to the journal pertain.

1                                    **Arabia-Eurasia collision and the forcing**  
2                                    **of mid Cenozoic global cooling**

3

4                                    Mark B. Allen\* and Howard A. Armstrong

5                                    *Department of Earth Sciences, Durham University, Durham, DH1 3LE, UK*

6                                    \* m.b.allen@durham.ac.uk

7

8                                    **Abstract**

9                                    The end of the Eocene greenhouse world was the most dramatic phase in the  
10                                    long-term cooling trend of the Cenozoic Era. Here we show that the Arabia-Eurasia  
11                                    collision and the closure of the Tethys ocean gateway began in the Late Eocene at ~35  
12                                    Ma, up to 25 million years earlier than in many reconstructions. We suggest that  
13                                    global cooling was forced by processes associated with the initial collision that  
14                                    reduced atmospheric CO<sub>2</sub>. These are: 1) waning volcanism across southwest Asia; 2)  
15                                    increased organic carbon storage in Paratethyan basins (e.g. Black Sea and South  
16                                    Caspian); 3) increased silicate weathering in the collision zone and, 4) a shift towards  
17                                    modern patterns of ocean currents, associated with increased vigour in circulation and  
18                                    organic productivity.

19                                    *Keywords:* Eocene; Oligocene; Tethys; Arabia-Eurasia collision; global cooling.

20

21                                    **1. Introduction**

22                                    Stable isotopic data for the early Cenozoic (Paleocene to Eocene) show a long-  
23                                    term pattern of cooling (Miller et al., 1987; Zachos et al., 2001; Tripathi et al., 2003)  
24                                    followed by the rapid expansion of the Antarctic continental ice sheet in the latest  
25                                    Eocene to earliest Oligocene (Ditchfield et al., 1994; Zachos et al., 2001). The latter

26 event, Oi-1, represents a 400 kyr-long glacial, initiated by reorganisation of the  
27 ocean/climate system. This is evidenced by global shifts in the distribution of marine  
28 biogenic sediments, including a ~1 km deepening of the calcite compensation depth  
29 (CCD) (Coxall et al., 2005) and an overall increase in ocean fertility (Baldauf and  
30 Barron, 1990; Salamy and Zachos, 1999; Thomas et al., 2000). A sharp positive  
31 carbon isotope excursion (~0.5 ‰) indicates a significant perturbation in the global  
32 carbon cycle (Zachos et al., 2001). High deep sea  $\delta^{18}\text{O}$  values (~2.5 ‰) during this  
33 event indicate permanent ice sheets, ~50% the size of the present day Antarctica ice  
34 sheet (Zachos et al., 2001). Significant cool-water upwelling during Oi-1 (Kennett and  
35 Barker, 1990; Barron et al., 1991; Diester-Haass, 1996; Salamy and Zachos, 1999;  
36 Exon et al., 2002) is supported by a pattern of declining biotic diversity among marine  
37 micro-invertebrates and dinoflagellates (Cifelli, 1969; Corliss, 1979; Benson et al.,  
38 1984), diversification of the diatoms (Katz et al., 2004) and a widespread change from  
39 carbonate (calcareous nannoplankton, foraminifers) to biosiliceous (diatom) oozes  
40 along the Antarctic margin. Oi-1 also coincides with a shift in continental floral belts  
41 (Frakes et al., 1992) and aridification and cooling in continental interiors Dupont-  
42 Nivet et al., 2007; Zanazzi et al., 2007).

43 The causes of the Oi-1 glaciation remain contentious and have hitherto focused  
44 on drivers from the southern high latitudes. Two first order causal hypotheses  
45 dominate thinking on mid Cenozoic climate change: 1) opening of ocean gateways  
46 separating Antarctica from other continents (Kennett, 1977); 2) reduction of  
47 atmospheric  $\text{CO}_2$  levels (DeConto and Pollard, 2003). Both hypotheses have caveats.  
48 Recent models indicate that changes in oceanic heat transport as the result of  
49 Antarctic isolation were too small to initiate Antarctic glaciation (Huber and Nof,  
50 2006). Also, the precise timing of circum-Antarctic gateways is controversial (Pfuhl

51 and McCave, 2005; Scher and Martin, 2006; Livermore et al., 2007). End Eocene  
52 decline in atmospheric CO<sub>2</sub> is supported by proxy data (Pagani et al., 2005), but this  
53 leads to the question: what caused the decline?

54 Different lines of evidence indicates that initial collision of the Arabian and  
55 Eurasian plates and closure of the Tethys Ocean took place at ~35 Ma (Late Eocene),  
56 up to 25 million years earlier than in many plate tectonic or oceanographic  
57 reconstructions (Woodruff and Savin, 1989; McQuarrie et al., 2003; Guest et al.,  
58 2006), but consistent with geologic data from across the collision zone, used in other  
59 reconstructions to argue for an Eocene age (Hempton, 1985; Vincent et al., 2005;  
60 Jassim and Goff, 2006). This collision caused constriction of the Tethys Gateway,  
61 which previously linked the Indian and Atlantic oceans (Fig. 1). We hypothesize that  
62 this event caused large-scale, multiple feedbacks in the carbon cycle that promoted  
63 global cooling and the Oi-1 glaciation.

64

## 65 **2. Date of initial Arabia-Eurasia continental collision**

66 There is considerable evidence for a Late Eocene (~35 Ma) age for the initial  
67 Arabia-Eurasia collision and elimination of intervening Tethyan oceanic crust (Figs 2  
68 and 3). Data include the timing of the following: compressional deformation, major  
69 surface uplift, exhumation, non-deposition or angular unconformities; sediment  
70 provenance switches and onset of terrestrial sedimentation, changes in  
71 palaeobiogeography and the switch-off of arc magmatism. The data divide into  
72 geographical sets on either side of the original plate suture; key regions are  
73 summarised in Fig. 3. Note that Arabia was a promontory of the African plate before  
74 the opening of the Red Sea in the mid Cenozoic, after initial Arabia-Eurasia collision.

75 To the south of the Arabia-Eurasia suture zone much of the collision history is  
76 recorded in the tectono-stratigraphy of the Zagros Mountains in SW Iran and adjacent  
77 parts of Iraq and Turkey. A regional Late Eocene – Early Oligocene angular  
78 unconformity is recognised in the northeast of the Zagros (Hessami et al., 2001) (Fig.  
79 3), interpreted by these authors as the early record of collision in an incipient foreland  
80 basin. Over much of the Zagros, Oligocene deposition was dominated by shallow  
81 marine carbonates of the Asmari Formation and its equivalents (Nadjafi et al., 2004),  
82 but approaching the suture to the northeast the carbonates are replaced by sandstones  
83 of the Razak Formation, shed from the region of the suture zone (Beydoun et al.,  
84 1992). Close to the suture in southwest Iran, in the Kermanshah-Hamedan area, some  
85 of the thrusts in the Zagros are post-Late Eocene to pre-Early Miocene, and are  
86 unconformably overlain by Upper Oligocene – Lower Miocene conglomerates (Agard  
87 et al., 2005) (Fig. 3). The thrust stack contains both Eocene volcanics and sedimentary  
88 rocks of Eurasian affinity and Cretaceous sediments and ophiolites from the northeast  
89 side of the Arabian plate (Agard et al., 2005).

90 In northeast Iraq, Upper Eocene terrestrial clastics of the Gercus Formation  
91 unconformably overlie deformed Mesozoic strata (Dhannoun et al., 1988). These  
92 strata and their underlying unconformity indicate compressional deformation and at  
93 least local sub-aerial uplift and erosion of the northeast edge of the Arabian plate by  
94 the Late Eocene, and have been interpreted as indicators of initial continental collision  
95 at this time (Jassim and Goff, 2006).

96 At the eastern end of the collision zone in northern Oman, a record of stable  
97 carbonate sedimentation from the latest Cretaceous – early Tertiary was terminated by  
98 Late Oligocene – Miocene folding (Searle, 1988). Collectively, these data record  
99 compressional deformation on the north Arabian margin from the Late Eocene

100 onwards (Fig. 3). Late Eocene compressional deformation also occurred at the  
101 western side of the collision zone, from Syria at least as far west as Algeria (Guiraud  
102 and Bosworth, 1999; Benaouali-Mebarek et al., 2006); it is not clear where effects of  
103 the Arabia-Eurasia collision pass westwards in to the rather enigmatic “Atlas” phase  
104 of deformation on the North African margin.

105         North of the suture, the Eurasian plate preserves a similar record of Late  
106 Eocene – Oligocene compressional deformation, uplift and associated sedimentation  
107 (Fig. 2). Close to the suture zone (Fig. 2), strata and igneous rocks as young as the  
108 Middle Eocene were folded and thrust, in places onto the Arabian plate, before being  
109 unconformably overlain by Oligocene sediments (Hempton, 1985; Yilmaz, 1993;  
110 Yigitbas and Yilmaz, 1996; Agard et al., 2005). Late Eocene thrusting in the Kyrenia  
111 Range of northern Cyprus is documented by deformed flysch and olistostrome  
112 deposits of this age, overlain unconformably by Lower Oligocene conglomerates and  
113 turbidites (Robertson and Woodcock, 1986). In the Berit region of southeast Turkey, a  
114 mid Eocene to earliest Miocene melange incorporates material derived from the  
115 Eurasian margin and is overlain by Lower Miocene turbidites, indicating that the  
116 Arabian plate had underthrust Eurasia by the earliest Miocene (Robertson et al., 2004)  
117 (Fig. 3). Within south-central Turkey several sedimentary basins, including Ulukışla  
118 (Fig. 2), underwent Late Eocene compressional deformation, with folding, thrusting  
119 and exhumation of volcanic rocks, turbidites and other sedimentary rocks deposited  
120 during Paleocene – Middle Eocene extension (Clark and Robertson, 2005; Jaffey and  
121 Robertson, 2005) (Fig. 3).

122         Eocene strata in the NW Greater Caucasus were deformed, exhumed and  
123 eroded before the deposition of Oligocene clastics (Aleksin and Ratner, 1967)  
124 indicating at least local deformation in this region near to the Eocene-Oligocene

125 boundary (Fig. 3). Parts of the western Greater Caucasus were emergent by at least  
126 the Early Oligocene (Vincent et al., 2007). Upper Eocene olistostromes south of the  
127 Greater Caucasus are interpreted as the result of compressional deformation (Banks et  
128 al., 1997), while seismic data from the margins of the eastern Black Sea show  
129 compressional deformation in the Late Eocene (Robinson et al., 1996). Syn-  
130 sedimentary slumps accompanied deposition of Upper Eocene turbidites in the  
131 Talysh, at the western margin of the South Caspian Basin (Vincent et al., 2005) (Fig.  
132 3). These relatively fine-grained marine strata are overlain by a coarsening-upwards  
133 Oligocene succession that includes boulder-scale conglomerates. This volcanic-free  
134 stratigraphy superseded a pre-late Eocene deep marine succession with abundant  
135 volcanism, including pillow basalts and tuffs. The Alborz range of northern Iran  
136 switched from a Middle Eocene depocentre, including turbidites and tuffs, into an  
137 emergent range by the early Oligocene (Stöcklin, 1974; Anell et al., 1975;  
138 Alavi, 1996; Guest et al., 2006,) (Fig. 3). Late Eocene – Oligocene deformation  
139 therefore occurred far to the north of the suture, suggesting that deformation  
140 propagated rapidly into the interior of Eurasia at the time of initial plate collision  
141 (Figs 2 and 3) (Robinson et al., 1996; Banks et al., 1997; Vincent et al., 2005; Vincent  
142 et al., 2007).

143 A Late Eocene initial collision is consistent with faunal data. There was  
144 progressive creation of separate Mediterranean and Indian Ocean marine realms, and  
145 migration of Eurasian and African/Arabian non-marine faunas (Harzhauser et al.,  
146 2002; Kappelman et al., 2003; Harzhauser et al., 2007). This is demonstrated by the  
147 tridacnine and strombid bivalves (Harzhauser et al., 2007), which show  
148 biogeographical divergence in the Oligocene. Gastropod assemblages also define two  
149 separate Tethys sub-provinces during the Oligocene, with an ill-defined boundary

150 within Iran and a rapid increase in endemism in the early Miocene (Harzhauser et al.,  
151 2002). The influx of Eurasian mammals into Africa indicates a land connection  
152 between Africa-Arabia and Eurasia existed by the Oligocene-Miocene boundary  
153 (Kappelman et al., 2003).

154 Tethyan sections at the Eocene-Oligocene transition show coeval faunal  
155 overturn in benthic foraminifera, accompanied by decreasing ventilation, preceding an  
156 increased intensity of abyssal circulation associated with the initial entry of bottom  
157 waters (likely to be North Atlantic Deep Water, NADW) and bolivinid/uvigerinid  
158 planktonic foraminifera blooms along the northern Tethys margin (Barbieri et al.,  
159 2003).

160

### 161 **3. Collision, the carbon cycle and oceanography**

162 Late Eocene closure of Tethys was coincident with declining  $p\text{CO}_2$  levels  
163 (Pagani et al., 2005), implicated as a major driver for global cooling and Antarctic  
164 glaciation (DeConto and Pollard, 2003). We propose four potential mechanisms for  
165 reducing  $p\text{CO}_2$  associated with initial Arabia-Eurasia collision and its effects on  
166 carbon fluxes and/or oceanographic circulation: decline of arc magmatism; storage of  
167 organic carbon in sedimentary basins; increased silicate weathering; stimulation of  
168 more vigorous, meridional ocean currents.

169

#### 170 *3.1. Declining Eocene arc magmatism in southwest Eurasia.*

171 Before the Arabia-Eurasia collision the Eurasian continental margin  
172 experienced arc magmatism as the result of the northwards subduction of Tethyan  
173 (strictly, Neo-Tethyan) oceanic crust. This magmatism provides a time constraint on  
174 the maximum likely age for initial continental collision, and would have been a net



175 source of atmospheric CO<sub>2</sub>. Across much of Iran and Turkey and adjacent areas there  
176 was a highly productive magmatic arc/back-arc system between ~50 and ~35 Ma.  
177 Magmatism was coincident with the renewal of northern motion of Africa-Arabia  
178 with respect to Eurasia, after a hiatus between 75 and 49 Ma (Dewey et al., 1989).  
179 Peak magmatism occurred in the Middle Eocene, close to 40 Ma, at which time  
180 volcanic successions accumulated at a rate of ~1.8 mm/yr, reached 4-8 km in  
181 thickness and occurred across an area of >2 million km<sup>2</sup> (Amidi et al., 1984; Kazmin  
182 et al., 1986; Brunet et al., 2003; McQuarrie et al., 2003; Ramezani and Tucker, 2003;  
183 Alpaslan et al., 2004; Vincent et al., 2005; Arslan and Aslan, 2006; Fig. 4). In detail,  
184 at least 4 km of intermediate-acidic volcanics are intercalated with mid-Eocene  
185 Nummulitic limestones in the Urumieh-Dokhtar arc in Iran (Berberian et al., 1982).  
186 Eight kilometres of mainly Middle Eocene volcanics and volcanogenic turbidites are  
187 recorded from the Talysh, adjacent to the South Caspian Basin (Vincent et al., 2005).  
188 Five km of Eocene andesitic volcanics and deep water clastics were deposited in the  
189 Alborz Mountains (Stöcklin, 1974; Alavi, 1996). Volcanism waned in the Late  
190 Eocene and there was little activity in the Oligocene (Fig. 4), though minor and  
191 sporadic magmatism has continued to the present day over much of the collision zone  
192 (Pearce et al., 1990).

193 Declining arc magmatism in the Late Eocene is consistent with the early  
194 deformation history of the collision zone (Fig. 2), whereby Late Eocene initial  
195 collision of the Arabian and Eurasian plates terminated oceanic subduction, ended  
196 back-arc continental extension across southwest Asia (Vincent et al., 2005) and  
197 generated compressional deformation and surface uplift. Abundant Middle Eocene arc  
198 magmatism across SW Asia would have promoted high atmospheric CO<sub>2</sub> levels,  
199 although the precise amount is not known. This highly productive arc coincides with

200 the Middle Eocene climatic optimum, previously attributed to an unspecified rise in  
201 ridge or arc magmatism (Bohaty and Zachos, 2003). Conversely, the sharp reduction  
202 in arc magmatism, brought about by initial Arabia-Eurasia collision, would have  
203 reduced CO<sub>2</sub> degassing into the atmosphere, and so acted to reduce global  
204 temperatures.

205

### 206 *3.2. Isolation of Paratethys and organic carbon storage.*

207 A new oceanographic configuration formed between the Alps and the Aral Sea  
208 during the Late Eocene and Oligocene (Veto, 1987; Jones and Simmons, 1997; Rögl,  
209 1999; Fig. 4). The basins were isolated from the global circulation, were prone to  
210 anoxia, and are collectively referred to as Paratethys or the Paratethyan basins. In the  
211 South Caspian and Black Sea basins the depocentres were located over blocks of  
212 highly attenuated continental crust or even oceanic crust (Finetti et al., 1988; Mangino  
213 and Priestley, 1998). These basement blocks are products of Mesozoic or early  
214 Cenozoic extension across southwestern Asia. Upper Eocene and Oligocene strata are  
215 commonly mud-prone and organic-rich across the region (Robinson et al., 1996;  
216 Vincent et al., 2005). Such organic-rich mudrocks are the main hydrocarbon source  
217 rock for the prolific oil fields of the Carpathians and South Caspian Basin, and are the  
218 main potential source rock in the eastern Black Sea. Total organic carbon (TOC)  
219 values reach 14% for the 2000 m thick Maykop Suite in the South Caspian Basin  
220 (Robinson et al., 1996; Katz et al., 2000). In the ~1000 m thick coeval strata of the  
221 Greater Caucasus, estimated average TOC values are ~1.5 to 2%. Typical thicknesses  
222 for the age equivalent Menilite Formation in eastern Europe are ~300 m, with average  
223 TOC of 2% (Veto, 1987). Based on these estimates of stratal thicknesses, extents and

224 average TOC, we estimate total organic sedimentary carbon in the combined Maykop  
225 and Menilite units at  $60 \times 10^{12}$  T.

226 Our estimate for organic carbon stored in the uppermost Eocene-Oligocene  
227 strata of the Paratethyan basins corresponds to an average deposition rate of  $\sim 6 \times 10^{12}$   
228 T per Ma through this interval, equivalent to  $\sim 12\%$  of the estimated global organic  
229 carbon flux in the late Paleogene (Raymo, 1994). This flux is a crude estimate, given  
230 that the distribution of organic carbon within the succession is poorly known but  
231 unlikely to be even. The overall effect of the carbon drawdown would have  
232 suppressed atmospheric  $\text{CO}_2$  levels throughout the latest Eocene and Oligocene.

233

### 234 *3.3. Increased silicate weathering.*

235 Continental collision and increased sub-aerial erosion in newly elevated areas  
236 would enhance low latitude silicate weathering (Raymo and Ruddiman, 1992), which  
237 in turn promotes  $\text{CO}_2$  drawdown from the atmosphere by reactions that can be  
238 summarised as:

239



241

242 Evidence for exposure and increased erosion comes from the presence of non-  
243 marine clastics or uplifted areas across large parts of the Arabia-Eurasia collision zone  
244 from the Late Eocene onwards. The precise contribution to global  $\text{CO}_2$  drawdown  
245 from silicate weathering in the collision zone is difficult to quantify, and likely to  
246 have been small given the area and likely rates involved when compared with global  
247 rates, but it acted in the right sense to promote climatic cooling. Enhanced weathering

248 and erosion could also help account for the increase in the oceanic  $^{87}\text{Sr}/^{86}\text{Sr}$  in the  
249 Late Eocene (Richter et al., 1992; Mead and Hodell, 1995).

250

### 251 3.4. Oceanographic changes.

252 Closure of Tethys resulted in a restructuring of Indian and Atlantic Ocean  
253 currents, closer to a modern pattern of ocean circulation and upwelling (Fig. 1). In the  
254 Cretaceous to Eocene (the “Proteus Ocean” of Kennett and Barker, 1990) low latitude  
255 surface currents were dominated by the circum-global westwards flow from the Indian  
256 Ocean to the Pacific via the Tethys and Panama gateways (Bush, 1997; Hallam, 1969;  
257 Huber and Sloan, 2001; Fig. 1). At about 37.5 Ma circum-equatorial surface water  
258 was directed southwards in the Indian Ocean via the Agulhas Current, as a result of  
259 the constricting Tethys Gateway (Diekmann et al., 2004). This current is a possible  
260 source of the moisture thought to be a critical element in maintaining a large mid  
261 Cenozoic Antarctic ice sheet (Zachos et al., 2001). Within the western Tethys  
262 (Mediterranean) region there was an increased intensity of abyssal circulation  
263 associated with the initial entry of NADW across the Eocene-Oligocene transition  
264 (Barbieri et al., 2003). Influx of cold corrosive deep water at ~34 Ma was a likely  
265 cause of marked faunal overturn in benthic foraminifera (Coccioni and Galeotti,  
266 2003). Contourite deposition began in Cyprus at ~36 Ma (Kahler and Stow, 1998),  
267 also indicating increased ocean current vigour.

268 Stable and Nd isotope data show that a marine connection between the Indian  
269 and Atlantic oceans persisted into the Miocene (Woodruff and Savin, 1989; Stille et  
270 al., 1996), but as argued here, this seaway cannot have been floored by oceanic crust.

271 Tethys closure was just one aspect of mid Cenozoic plate re-configuration and  
272 oceanographic change. The widening North Atlantic led to the start of NADW at ~35

273 Ma (Wold, 1994; Zachos et al., 2001; Via and Thomas, 2006). Atlantic circulation  
274 patterns similar to the present day were established at this time (Via and Thomas,  
275 2006). Although the precise timing for the opening of Antarctic gateways is still  
276 debated, the trend towards isolation is clear in plate reconstructions (Livermore et al.,  
277 2007). Likewise, Mediterranean tectonics involved rapid compressional and  
278 extensional events in the early Cenozoic, in the context of the overall convergence of  
279 Africa and Europe (Dewey et al., 1989; Rubatto et al., 1998), but without complete  
280 severance of the Tethyan seaway west of Arabia.

281 Oceanographic changes have been implicated in global climate change via  
282 increased upwelling, organic productivity and hence atmospheric CO<sub>2</sub> drawdown  
283 (Diester-Haass and Zahn, 1996, 2001; Schumacher and Lazarus, 2004; Anderson and  
284 Delaney, 2005). Our point is that Late Eocene Tethys closure is a previously  
285 unappreciated factor in this global re-organisation.

286

#### 287 **4. Conclusions**

288 Oceanographic, plate tectonic and climatic modelling studies commonly take  
289 ~14 to 10 Ma (mid Miocene) as both the end of the Tethys connection between the  
290 Indian and Atlantic oceans and the initial Arabia-Eurasia collision (Woodruff and  
291 Savin, 1989; McQuarrie et al., 2003). Our interpretation of the collision is that the last  
292 oceanic plate separation between Arabia and Eurasia was in the Late Eocene at ~35  
293 Ma (Fig. 1), agreeing with previous estimates for this age based on geological patterns  
294 within the collision zone (Jassim and Goff, 2006; Vincent et al., 2007).

295 Initial Arabia-Eurasia plate collision and closure of the Tethys Ocean provides  
296 four complementary mechanisms for reducing atmospheric CO<sub>2</sub> and global cooling:  
297 1) the waning of pre-collision arc magmatism, 2) storage of organic carbon in the

298 Paratethyan basins, 3) an increase in silicate weathering, 4) re-organisation of ocean  
299 currents, consistent with global end Eocene increases in ocean current vigour, organic  
300 productivity and hence CO<sub>2</sub> drawdown. We contend that all these mechanisms acted  
301 together to help take the Earth across a threshold into the icehouse world at the Oi-1  
302 event.

303

#### 304 **Acknowledgements**

305 We thank Steve Vincent, Mike Simmons, Howie Scher, James Baldini and  
306 Glenn Milne for discussions. Laurent Jolivet and Eduardo Garzanti provided helpful  
307 reviews. Supported by Durham University research project R050451.

308

#### 309 **Figures**

310 Fig. 1. Palaeogeographic and oceanographic reconstructions before and after the  
311 demise of the Tethys Ocean gateway. **(A)** Eocene period, with westerly transport of  
312 warm Indian Ocean water into the Atlantic via Tethys. **(B)** Oligocene, with  
313 connection between the Indian and Atlantic oceans impeded by the Arabia-Eurasia  
314 collision zone. Ocean currents derived from Bush (1997); Diekmann et al. (2004);  
315 Kennett and Barker (1990); Stille et al. (1996); Thomas et al. (2003); Via and Thomas  
316 (2006); von der Heydt and Dijkstra (2006).

317

318 Fig. 2. Present topography of the Arabia-Eurasia collision, location map for regions  
319 summarised in Fig. 3, and position of the Arabia-Eurasia suture.

320

321 Fig. 3. Summary tectonostratigraphy for localities showing Late Eocene – Oligocene  
322 deformation and/or uplift. Localities shown on Fig. 2. Derived from: Stöcklin, (1974);

323 Annells et al., (1975); Searle, (1988); Banks et al., (1997); Beydoun et al., (1992);  
324 Hessami et al., (2001); Agard et al., (2005); Clark and Robertson, (2005); Vincent et  
325 al., (2005, 2007); Guest et al., (2006); Boulton and Robertson, (2006); Jassim and  
326 Goff, (2006); Robertson et al., (2006).

327

328 Fig. 4. Comparison of the present distribution of (A) Eocene and (B) Oligocene  
329 magmatic rocks across southwest Asia. Derived from principally from Emami et al.,  
330 (1993); Şenel (2002). Other sources summarised in Vincent et al. (2005). (B) also  
331 shows the extent of Oligocene sediments from the Paratethyan basins (Veto, 1987).

332

### 333 **References**

334 Agard, P., Omrani, J., Jolivet, L., Mouthereau, F., 2005. Convergence history across  
335 Zagros (Iran): constraints from collisional and earlier deformation. *International*  
336 *Journal of Earth Sciences* 94, 401-419.

337 Alavi, M., 1996. Tectonostratigraphic synthesis and structural style of the Alborz  
338 mountain system in northern Iran. *Journal of Geodynamics* 21, 1-33.

339 Aleksin, A.G., Ratner, V.Y., 1967. Oil and gas fields of the hydrocarbon basins of  
340 Russian SFSR, Ukrainian SSR and Kazakh SSR. Explanatory notes to the  
341 album, Nauchno-Issledovatel'skaya Laboratoriya Geologii Zarubezhnykh Stran,  
342 215pp.

343 Alpaslan, M., Frei, R., Boztug, D., Kurt, M.A., Temel, A., 2004. Geochemical and  
344 Pb-Sr-Nd isotopic constraints indicating an enriched-mantle source for late  
345 Cretaceous to early Tertiary volcanism, Central Anatolia, Turkey. *International*  
346 *Geology Review* 46, 1022-1041.

- 347 Amidi, S.M., Emami, M.H., Michel, R., 1984. Alkaline character of Eocene  
348 volcanism in the middle part of Central Iran and its geodynamic situation.  
349 *Geologische Rundschau* 73, 917-932.
- 350 Anderson, L.D., Delaney, M.L., 2005. Middle Eocene to early Oligocene  
351 paleoceanography from Agulhas Ridge, Southern Ocean (Ocean Drilling  
352 Program Leg 177, Site 1090). *Paleoceanography* 20, Art. No. PA1013, doi  
353 10.1029/2004PA001043.
- 354 Annells, R.N., Arthurton, R.S., Bazley, R.A., Davies, R.G., 1975. Explanatory text of  
355 the Qazvin and Rasht Quadrangles Map, E3 and E4. Geological Survey of Iran  
356 94pp.
- 357 Arslan, A., Aslan, Z., 2006. Mineralogy, petrography and whole-rock geochemistry of  
358 the Tertiary granitic intrusions in the Eastern Pontides, Turkey. *Journal of Asian  
359 Earth Sciences* 27, 177-193.
- 360 Baldauf, J.G. , Barron, J.A., 1990. Evolution of biosiliceous sedimentation patterns  
361 Eocene through Quaternary: paleoceanographic response to polar cooling. In: U.  
362 Bleil and J. Thiede (Editors), *Geological history of the Polar Oceans: Arctic  
363 versus Antarctic*. Kluwer, Dordrecht, pp. 575-607.
- 364 Banks, C.J., Robinson, A.G., Williams, M.P., 1997. Structure and regional tectonics  
365 of the Achara-Trialet fold belt and the adjacent Rioni and Kartli foreland basins,  
366 republic of Georgia. In: A. Robinson (Editor), *Regional and petroleum geology  
367 of the Black Sea and surrounding region*. AAPG Memoir 68 pp. 331-346.
- 368 Barbieri, R., Benjamini, C., Monechi, S., Reale, V., 2003. Stratigraphy and benthic  
369 foraminiferal events across the Middle-Late Eocene transition in the Western  
370 Negev., Israel. In: D.R. Prothero, L.C. Ivany and E.A. Nesbitt (Editors), *From*



- 371 greenhouse to icehouse: The marine Eocene-Oligocene transition. Columbia  
372 University Press, New York, pp. 453-471.
- 373 Barron, J.A., Baldauf, J.G., Barrera, E., Caulet, J.P., Huber, B.T., Keating, B.H.,  
374 Lazarus, D., Sakai, H., Thierstein, H. R., Wei, W., 1991. Biochronologic and  
375 magnetostratigraphic synthesis of Leg 119 sediments from the Kerguelen Plateau  
376 and Prydz Bay, Antarctica. Proceedings of the Ocean Drilling Program, Scientific  
377 Results, 119, 813-847.
- 378 Benaouali-Mebarek, N., de Lamotte, D.F., Roca, E., Bracene, R., Faure, J.L., Sassi,  
379 W., Roure, F., 2006. Post-Cretaceous kinematics of the Atlas and Tell systems  
380 in central Algeria: Early foreland folding and subduction-related deformation.  
381 *Comptes Rendus Geoscience* 338, 115-125.
- 382 Benson, R.H., Chapman, R.E., Deck, L.T., 1984. Paleooceanographic events and deep-  
383 sea ostracodes. *Science* 224, 1334-1336.
- 384 Berberian, F., Muir, I.D., Pankhurst, R.J., Berberian, M., 1982. Late Cretaceous and  
385 early Miocene Andean-type plutonic activity in northern Makran and Central  
386 Iran. *Journal of the Geological Society* 139, 605-614.
- 387 Beydoun, Z.R., Hughes Clarke, M.W., Stoneley, R., 1992. Petroleum in the Zagros  
388 Basin: a late Tertiary foreland basin overprinted onto the outer edge of a vast  
389 hydrocarbon-rich Paleozoic-Mesozoic passive-margin shelf. In: R. MacQueen  
390 and D. Leckie (Editors), *Foreland Basins and Foldbelts*. AAPG Memoir 55, pp.  
391 309-339.
- 392 Bohaty, S.M., Zachos, J.C., 2003. Significant Southern Ocean warming event in the  
393 late middle Eocene. *Geology* 31, 1017-1020.
- 394 Boulton, S.J., Robertson, A.H.F., 2006. Tectonic and sedimentary evolution of the  
395 Cenozoic Hatay Graben, Southern Turkey: a two-phase model for graben

- 396 evolution. In: A.H.F. Robertson and D. Mountrakis (Editors), *Tectonic*  
397 *Development of the Eastern Mediterranean Region*. Geological Society of  
398 London, Special Publications 260, London, pp. 613-634.
- 399 Brunet, M.F., Korotaev, M.V., Ershov, A.V., Nikishin, A.M., 2003. The South  
400 Caspian Basin: a review of its evolution from subsidence modelling.  
401 *Sedimentary Geology* 156, 119-148.
- 402 Bush, A.B.G., 1997. Numerical simulation of the Cretaceous Tethys circumglobal  
403 current. *Science*, 275 807-810.
- 404 Cifelli, R., 1969. Radiation of Cenozoic planktonic foraminifera. *Systematic Zoology*  
405 18, 154-168.
- 406 Clark, M., Robertson, A., 2005. Uppermost Cretaceous-Lower Tertiary Ulukisla  
407 Basin, south- central Turkey: sedimentary evolution of part of a unified basin  
408 complex within an evolving Neotethyan suture zone. *Sedimentary Geology* 173,  
409 15-51.
- 410 Coccioni, R., Galeotti, S., 2003. Deep-water benthic foraminiferal events from the  
411 Massignano Eocene/Oligocene boundary stratotype, central Italy. In: D.R.  
412 Prothero, L.C. Ivany and E.A. Nesbitt (Editors), *From Greenhouse to Icehouse:*  
413 *The Marine Eocene - Oligocene transition*. Columbia University Press, New  
414 York, pp. 438-453.
- 415 Corliss, B.H., 1979. Response of the deep sea benthic foraminifera to development of  
416 the psychrosphere near the Eocene-Oligocene boundary. *Nature* 282, 63-65.
- 417 Coxall, H.K., Wilson, P.A., Palike, H., Lear, C.H., Backman, J., 2005. Rapid stepwise  
418 onset of Antarctic glaciation and deeper calcite compensation in the Pacific  
419 Ocean. *Nature* 433, 53-57.

- 420 DeConto, R.M., Pollard, D., 2003. Rapid Cenozoic glaciation of Antarctica induced  
421 by declining atmospheric CO<sub>2</sub>. *Nature* 421, 245-249.
- 422 Dewey, J.F., Helman, M.L., Turco, E., Hutton, D.H.W., Knott, S.D., 1989.  
423 Kinematics of the western Mediterranean. In: M.P. Coward, D. Dietrich and  
424 R.G. Park (Editors), *Alpine Tectonics*. Special Publication of the Geological  
425 Society, London, pp. 265-283.
- 426 Dhannoun, H.Y., Aldabbagh, S.M.A., Hasso, A.A., 1988. The Geochemistry of the  
427 Gercus Red-Bed Formation of Northeast Iraq. *Chemical Geology* 69, 87-93.
- 428 Diekmann, B., Kuhn, G., Gersonde, R., Mackensen, A., 2004. Middle Eocene to early  
429 Miocene environmental changes in the sub-Antarctic Southern Ocean: evidence  
430 from biogenic and terrigenous depositional patterns at ODP Site 1090. *Global  
431 and Planetary Change* 40, 295-313.
- 432 Diester-Haass, L., Zahn, R., 2001. Paleoproductivity increase at the Eocene-  
433 Oligocene climatic transition: ODP/DSDP sites 763 and 592. *Palaeogeography  
434 Palaeoclimatology Palaeoecology* 172, 153-170.
- 435 Diester-Haass, L., 1996. Late Eocene-Oligocene paleoceanography in the southern  
436 Indian Ocean (ODP Site 744). *Marine Geology* 130, 99-119.
- 437 Diester-Haass, L., Zahn, R., 1996. Eocene-Oligocene transition in the Southern  
438 Ocean: History of water mass circulation and biological productivity. *Geology*  
439 24, 163-166.
- 440 Ditchfield, P.W., Marshall, J.D., Pirrie, D., 1994. High latitude palaeotemperature  
441 variation: New data from the Tithonian to Eocene of James Ross Island,  
442 Antarctica. *Palaeogeography, Palaeoclimatology, Palaeoecology* 107, 79-101.

- 443 Dupont-Nivet, G. Krijgsman, W., Langereis, C.G., Abels, H.A., Dai, S., Fang, X.M.,  
444 2007. Tibetan plateau aridification linked to global cooling at the Eocene-  
445 Oligocene transition. *Nature* 445, 635-638.
- 446 Emami, M.H., Sadeghi, M.M.M., Omrani, S.J., 1993. Magmatic map of Iran.  
447 Geological Survey of Iran, Tehran.
- 448 Exon, N.F. and 28 others, 2002. Drilling reveals climatic consequences of Tasmanian  
449 gateway opening. *Eos, Transactions American Geophysical Union* 83, 253-259.
- 450 Frakes, L.A., Francis, J.E., Sykes, J.I., 1992. *Climate Modes of the Phanerozoic*.  
451 Cambridge University Press, Cambridge, 274 pp.
- 452 Finetti, I., Bricchi, G., Del Ben, A., Pipan, M., Xuan, Z., 1988, Geophysical study of  
453 the Black Sea. *Bolletino di Geofisica Teorica ed Applicata* 30, 197-324.
- 454 Guest, B., Stockli, D.F., Grove, M., Axen, G.J., Lam, P.S., Hassanzadeh, J., 2006.  
455 Thermal histories from the central Alborz Mountains, northern Iran:  
456 Implications for the spatial and temporal distribution of deformation in northern  
457 Iran. *Geological Society of America Bulletin* 118, 1507-1521.
- 458 Guiraud, R., Bosworth, W., 1999. Phanerozoic geodynamic evolution of northeastern  
459 Africa and the northwestern Arabian platform. *Tectonophysics* 315, 73-108.
- 460 Hallam, A., 1969. Faunal realms and facies in the Jurassic. *Palaeontology* 12, 1-18.
- 461 Harzhauser, M., Piller, W.E., Steininger, F.F., 2002. Circum-Mediterranean Oligo-  
462 Miocene biogeographic evolution - the gastropods' point of view.  
463 *Palaeogeography Palaeoclimatology Palaeoecology* 183, 103-133.
- 464 Harzhauser, M., Kroh, A., Mandic, O., Piller, W.E., Gohlich, U., Reuter, M., Berning,  
465 B., 2007, Biogeographic responses to geodynamics: A key study all around the  
466 Oligo-Miocene Tethyan Seaway. *Zoologischer Anzeiger* 246, 241-256.

- 467 Hempton, M.R., 1985. Structure and deformation history of the Bitlis suture near  
468 Lake Hazar, southeastern Turkey. *Geological Society of America Bulletin* 96,  
469 233-243.
- 470 Hessami, K., Koyi, H.A., Talbot, C.J., Tabasi, H., Shabaniyan, E., 2001. Progressive  
471 unconformities within an evolving foreland fold-thrust belt, Zagros Mountains.  
472 *Journal of the Geological Society, London* 158, 969-981.
- 473 Huber, B.T., Sloan, L.C., 2001. Heat transport, deep waters, and thermal gradients:  
474 coupled simulation of an Eocene greenhouse climate. *Geophysical Research*  
475 *Letters* 28, 3481-3484.
- 476 Huber, M., Nof, D., 2006. The ocean circulation in the southern hemisphere and its  
477 climatic impacts in the Eocene. *Palaeogeography Palaeoclimatology*  
478 *Palaeoecology* 231, 9-28.
- 479 Jaffey, N., Robertson, A., 2005. Non-marine sedimentation associated with  
480 Oligocene-Recent exhumation and uplift of the central Taurus Mountains, S  
481 Turkey. *Sedimentary Geology* 73, 53-89.
- 482 Jassim, S.Z., Goff, J.C., 2006. Phanerozoic development of the northern Arabian  
483 Plate. In: S.Z. Jassim and J.C. Goff (Editors), *Geology of Iraq*. Dolin, Prague,  
484 pp. 32-44.
- 485 Jones, R.W., Simmons, M.D., 1997. A review of the stratigraphy of Eastern  
486 Paratethys (Oligocene-Holocene), with particular emphasis on the Black Sea. In:  
487 A. Robinson (Editor), *Regional and petroleum geology of the Black Sea and*  
488 *surrounding region*. AAPG Memoir 68, pp. 39-52.
- 489 Kahler, G., Stow, D.A.V., 1998. Turbidites and contourites of the Palaeogene Lefkara  
490 Formation, southern Cyprus. *Sedimentary Geology* 115, 215-231.

- 491 Kappelman, J. and 21 others, 2003. Oligocene mammals from Ethiopia and faunal  
492 exchange between Afro-Arabia and Eurasia. *Nature* 426, 549-552.
- 493 Katz, B., Richards, B., Long, D., Lawrence, W., 2000. A new look at the components  
494 of the petroleum system of the South Caspian Basin. *Journal of Petroleum*  
495 *Science and Engineering*, 28 161-182.
- 496 Katz, M.E., Finkel, Z.V., Grzebyk, D., Knoll, A.H., Falkowski, P.G., 2004.  
497 Evolutionary trajectories and biogeochemical impacts of marine eukaryotic  
498 phytoplankton. *Annual Review of Ecology and Evolutionary Systematics* 35,  
499 523-556.
- 500 Kazmin, V.G. Sborshchikov, I.M., Ricou, L.-E., Zonenshain, L.P., Boulin, J.,  
501 Knipper, A.L., 1986. Volcanic belts as markers of the Mesozoic-Cenozoic active  
502 margin of Eurasia. *Tectonophysics* 123, 123-152.
- 503 Kennett, J.P., 1977. Cenozoic evolution of Antarctic glaciation, the circum-Antarctic  
504 ocean and their impact on global paleoceanography. *Journal of Geophysical*  
505 *Research* 82, 843-860.
- 506 Kennett, J.P., Barker, P.F., 1990. Latest Cretaceous to Cenozoic climate and  
507 oceanographic developments in the Weddell Sea, Antarctica: an ocean drilling  
508 perspective. *Proceedings of the Ocean Drilling Program, Scientific Results* 113,  
509 937-960.
- 510 Livermore, R., Hillenbrand, C.D., Meredith, M., Eagles, G., 2007. Drake Passage and  
511 Cenozoic climate: An open and shut case? *Geochemistry Geophysics*  
512 *Geosystems* 8, art. no. Q01005, doi 10.1029/2005GC001224.
- 513 Mangino, S., Priestley, K., 1998, The crustal structure of the southern Caspian region.  
514 *Geophysical Journal International* 133, 630-648.

- 515 McQuarrie, N., Stock, J.M., Verdel, C., Wernicke, B., 2003. Cenozoic evolution of  
516 Neotethys and implications for the causes of plate motions. *Geophysical*  
517 *Research Letters* 30: art. no. 2036 doi 10.1029/2003GL017992.
- 518 Mead, G.A., Hodell, D.A., 1995. Controls on the Sr-87/Sr-86 composition of seawater  
519 from the Middle Eocene to Oligocene - Hole 689B, Maud Rise, Antarctica.  
520 *Paleoceanography* 10, 327-346.
- 521 Miller, K.G., Fairbanks, R.A., Mountain, G.S., 1987. Tertiary oxygen isotope  
522 synthesis, sea-level history and continental margin erosion. *Paleoceanography* 2,  
523 1-19.
- 524 Nadjafi, M., Mahboubi, A., Moussavi-Harami, R., Mirzaee, R., 2004. Depositional  
525 history and sequence stratigraphy of outcropping Tertiary carbonates in the  
526 Jahrum and Asmari formations, Shiraz area (SW Iran). *Journal of Petroleum*  
527 *Geology* 27, 179-190.
- 528 Pagani, M., Zachos, J.C., Freeman, K.H., Tipple, B., Bohaty, S., 2005. Marked  
529 decline in atmospheric carbon dioxide concentrations during the Paleogene.  
530 *Science* 309, 600-603.
- 531 Pearce, J.A., Bender, J. F., Delong, S. E., Kidd, W. S. F., Low, P. J., Guner, Y.,  
532 SaRöglu, F., Yilmaz, Y., Moorbath, S., Mitchell, J. G., 1990. Genesis of  
533 collision volcanism in eastern Anatolia, Turkey. *Journal of Volcanology and*  
534 *Geothermal Research* 44, 189-229.
- 535 Pfuhl, H.A., McCave, I.N., 2005. Evidence for late Oligocene establishment of the  
536 Antarctic Circumpolar Current. *Earth and Planetary Science Letters* 235, 715-  
537 728.

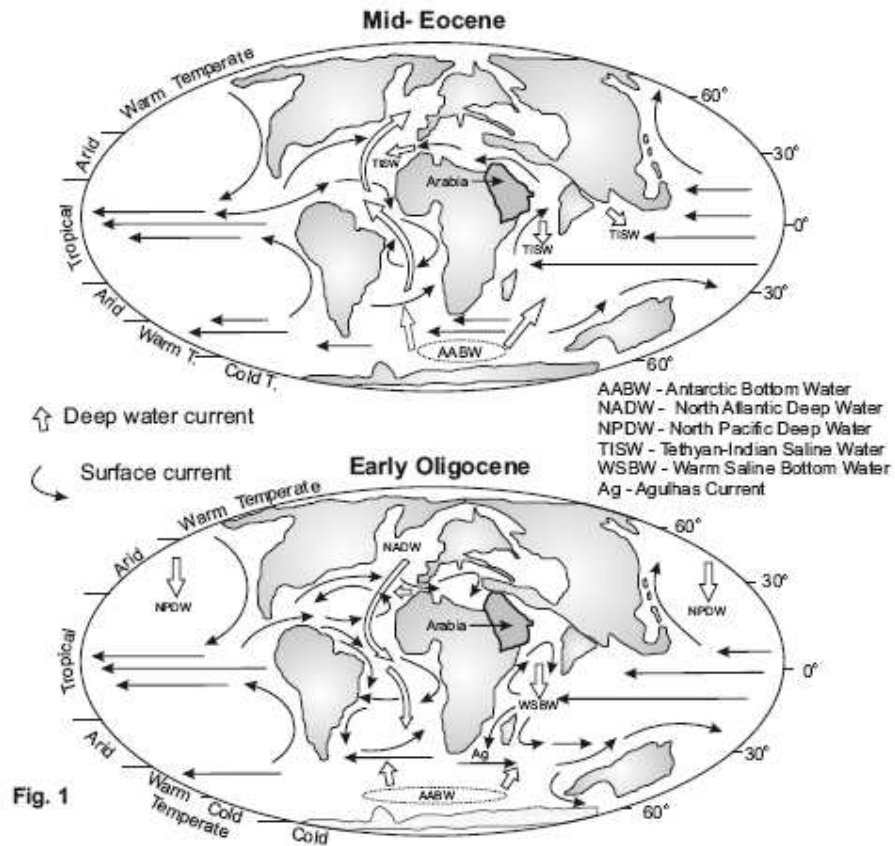
- 538 Ramezani, J., Tucker, R.D., 2003. The Saghand region, central Iran: U-Pb  
539 geochronology, petrogenesis and implications for Gondwana tectonics.  
540 American Journal of Science 303, 622-665.
- 541 Raymo, M.E., 1994. The Himalayas, organic-carbon burial, and climate in the  
542 Miocene. *Paleoceanography* 9, 399-404.
- 543 Raymo, M.E., Ruddiman, W.F., 1992. Tectonic forcing of late Cenozoic climate.  
544 *Nature* 359, 117-122.
- 545 Richter, F.M., Rowley, D.B., DePaolo, D.J., 1992. Sr isotope evolution of seawater -  
546 the role of tectonics. *Earth and Planetary Science Letters* 109, 11-23.
- 547 Robertson, A., Unlugenc, O.C., Inan, N., Tasli, K., 2004. The Misis-Andirin complex:  
548 a mid-tertiary melange related to late-stage subduction of the southern Neotethys  
549 in S Turkey. *Journal of Asian Earth Sciences* 22, 413-453.
- 550 Robertson, A.H.F., Ustaomer, T., Parlak, O., Unlugenc, U. C., Tasli, K., Inan, N.,  
551 2006. The Berit transect of the Tauride thrust belt, S Turkey: Late Cretaceous-  
552 Early Cenozoic accretionary/collisional processes related to closure of the  
553 Southern Neotethys. *Journal of Asian Earth Sciences*, 27, 108-145.
- 554 Robertson, A.H.F., Woodcock, N.H., 1986. The role of the Kyrenia Range lineament,  
555 Cyprus, in the geological evolution of the eastern Mediterranean area.  
556 *Philosophical Transactions of the Royal Society of London Series A-  
557 Mathematical Physical and Engineering Sciences* 317, 141-177.
- 558 Robinson, A., Rudat, J., Banks, C., Wiles, R., 1996. Petroleum geology of the Black  
559 Sea. *Marine and Petroleum Geology* 13, 195-223.
- 560 Rögl, F., 1999. Mediterranean and Paratethys. Facts and hypotheses of an Oligocene  
561 to Miocene paleogeography (short overview). *Geologica Carpathica* 50, 339-  
562 349.



- 563 Rubatto, D., Gebauer, D., Fanning, M., 1998, Jurassic formation and Eocene  
564 subduction of the Zermatt-Saas-Fee ophiolites: implications for the geodynamic  
565 evolution of the Central and Western Alps. *Contributions to Mineralogy and*  
566 *Petrology* 132, 269-287.
- 567 Salamy, K.A., Zachos, J.C., 1999. Latest Eocene-early Oligocene climate change and  
568 Southern Ocean fertility: Inferences from sediment accumulation and stable  
569 isotope data. *Palaeogeography Palaeoclimatology Palaeoecology* 145, 61-77.
- 570 Scher, H.D., Martin, E.E., 2006. Timing and climatic consequences of the opening of  
571 Drake Passage. *Science* 312, 428-430.
- 572 Schumacher, S., Lazarus, D., 2004. Regional differences in pelagic productivity in the  
573 late Eocene to early Oligocene - a comparison lower of southern high latitudes  
574 and longitudes. *Palaeogeography Palaeoclimatology Palaeoecology* 214, 243-  
575 263.
- 576 Searle, M.P., 1988. Structure of the Musandam Culmination (Sultanate-Of-Oman And  
577 United-Arab-Emirates) and the Straits of Hormuz Syntaxis. *Journal of the*  
578 *Geological Society* 145, 831-845.
- 579 Şenel, M., 2002. Geological map of Turkey. General Directorate of Mineral Research  
580 and Exploration, Ankara.
- 581 Stille, P., Steinmann, M., Riggs, S.R., 1996. Nd isotope evidence for the evolution of  
582 the paleocurrents in the Atlantic and Tethys Oceans during the past 180 Ma.  
583 *Earth and Planetary Science Letters* 144, 9-19.
- 584 Stöcklin, J., 1974. Northern Iran: Alborz mountains. In: A. Spencer (Editor),  
585 *Mesozoic-Cenozoic orogenic belts: data for orogenic studies. Special*  
586 *Publication of the Geological Society of London*, pp. 213-234.

- 587 Thomas, D.J., Bralower, T.J., Jones, C.E., 2003. Neodymium isotopic reconstruction  
588 of late Paleocene-early Eocene thermohaline circulation. *Earth and Planetary*  
589 *Science Letters* 209, 309-322.
- 590 Thomas, E., Zachos, J.C. , Bralower, T.J., 2000. Deep-sea environments on a warm  
591 Earth: Latest Paleocene–early Eocene. In: B.T. Huber, K.G. MacLeod and S.L.  
592 Wing (Editors), *Warm Climates in Earth History*. Cambridge University Press,  
593 New York, pp. 132-160.
- 594 Tripathi, A., Delaney, M.L., Zachos, J.C., Anderson, L.D., Kelly, D.C., Elderfield, H.,  
595 2003. Tropical sea surface temperature reconstructions for the early Paleogene  
596 using Mg/Ca ratios of planktonic foraminifera. *Paleoceanography* 18, art. no.  
597 1011, doi 10.1029/2003PA000937.
- 598 Veto, I., 1987. An Oligocene sink for organic-carbon - upwelling in the Paratethys.  
599 *Palaeogeography Palaeoclimatology Palaeoecology* 60, 143-153.
- 600 Via, R.K., Thomas, D.J., 2006. Evolution of Atlantic thermohaline circulation: Early  
601 Oligocene onset of deep-water production in the North Atlantic. *Geology* 34,  
602 441-444.
- 603 Vincent, S.J., Allen, M.B., Ismail-Zadeh, A.D., Flecker, R., Foland, K.A., Simmons,  
604 M.D. 2005. Insights from the Talysh of Azerbaijan into the Paleogene evolution  
605 of the South Caspian region. *Bulletin of the Geological Society of America* 117,  
606 1513-1533.
- 607 Vincent, S.J., Morton, A.C., Carter, A., Gibbs, S., Barabadze, T.G., 2007. Oligocene  
608 uplift of the Western Greater Caucasus: an effect of initial Arabia-Eurasia  
609 collision. *Terra Nova* 19, 160-166.

- 610 von der Heydt, A., Dijkstra, H.A., 2006. Effect of ocean gateways on the global ocean  
611 circulation in the late Oligocene and early Miocene. *Paleoceanography* 21, art.  
612 no. PA1101 doi:10.1029/2005PA001149.
- 613 Wold, C.N., 1994. Cenozoic sediment accumulation on drifts in the northern North  
614 Atlantic. *Paleoceanography* 9, 917-941.
- 615 Woodruff, F., Savin, S.M., 1989. Miocene deepwater oceanography.  
616 *Paleoceanography* 4, 87-140.
- 617 Yigitbas, E., Yilmaz, Y., 1996. New evidence and solution to the Maden Complex  
618 controversy of the Southeast Anatolian orogenic belt (Turkey). *Geologische*  
619 *Rundschau* 85, 250-263.
- 620 Yilmaz, Y., 1993. New evidence and model on the evolution of the southeast  
621 Anatolian orogen. *Bulletin of the Geological Society of America* 105, 251-271.
- 622 Zachos, J.C., Pagani, M., Sloan, E.T., Billups, K., 2001. Trends, rhythms, and  
623 aberrations in global climate 65 Ma to present. *Science* 292, 686-694.
- 624 Zanazzi, A., Kohn, M.J., MacFadden, B.J., Terry, D.O., 2007. Large temperature drop  
625 across the Eocene-Oligocene transition in central North America. *Nature* 445,  
626 639-642.



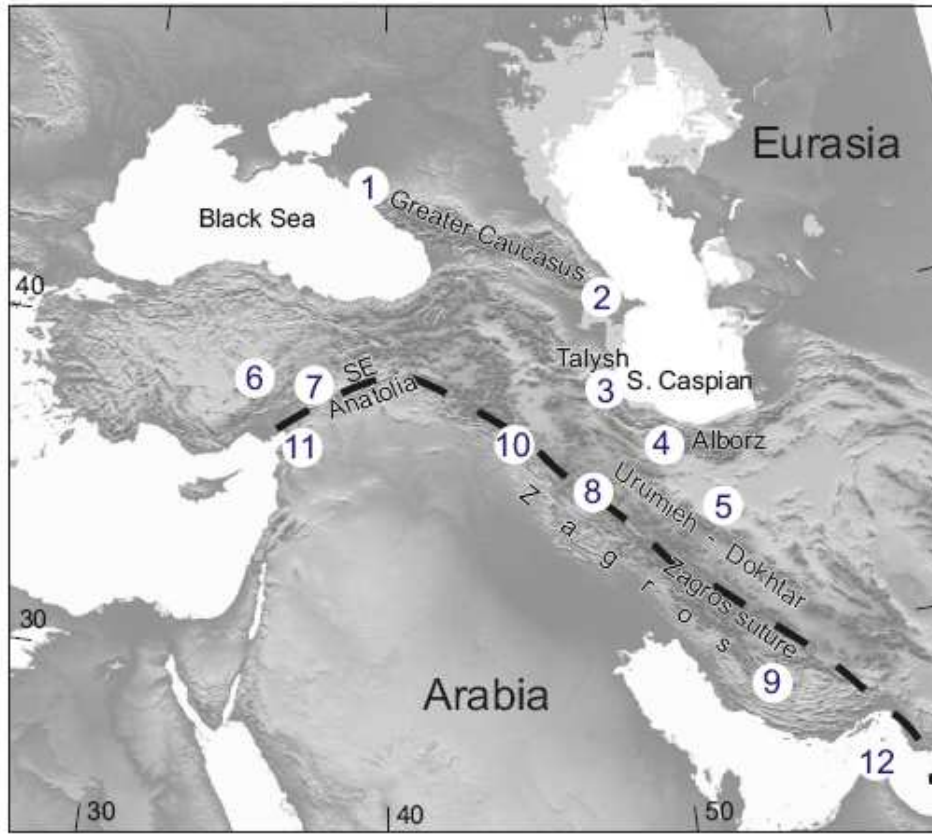


Fig. 2

628

ACC

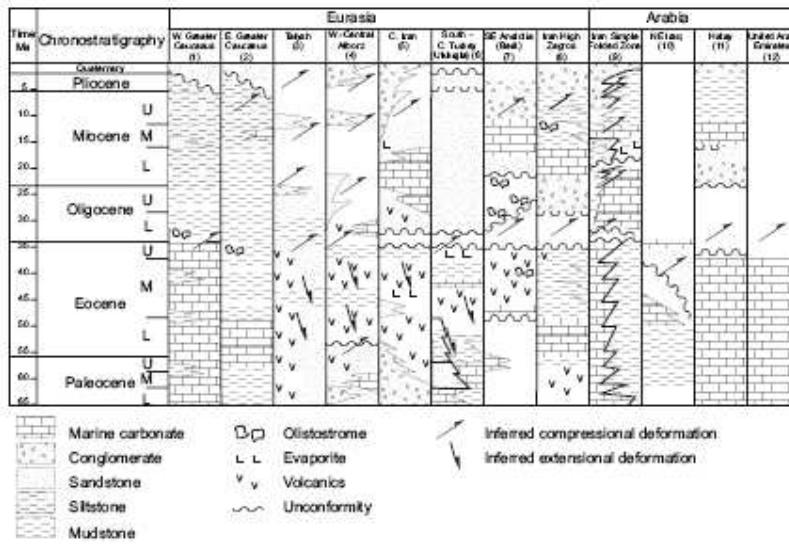
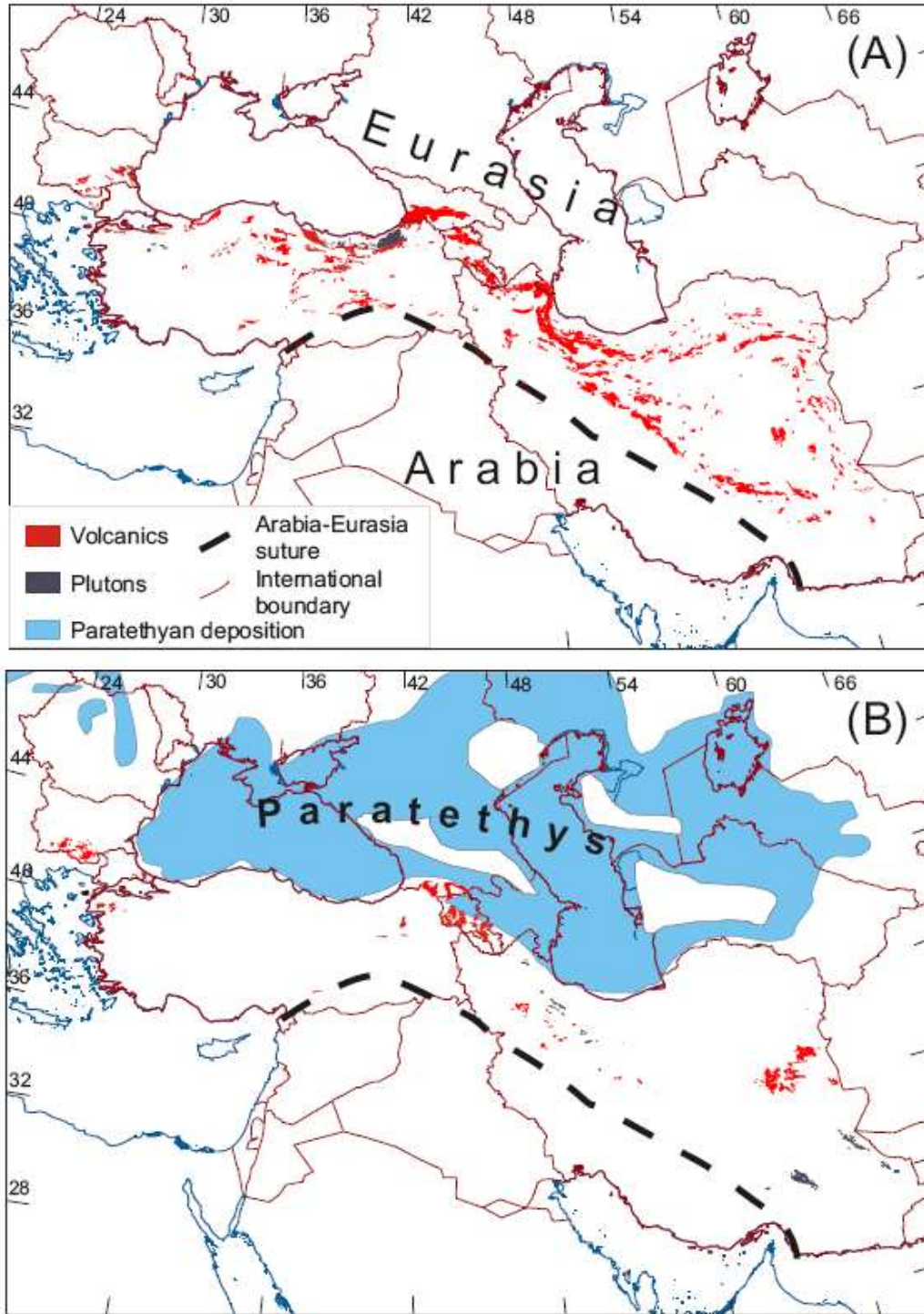


Fig. 3



630

Fig. 4